Available online at www.sciencedirect.com

ScienceDirect

Procedia Structural Integrity 28 (2020) 2032–2042

Structural Integrity Procedia

www.elsevier.com/locate/procedia

1st Virtual European Conference on Fracture

On kinetic model of damage development

I S Nikitin*, N G Burago, A D Nikitin and B A Stratula

Institute for computer aided design of RAS, 2-ya Brestskaya st., 123056, Moscow, Russia

Abstract

A complex kinetic model of damage development under cyclic loading is proposed to describe the process of fatigue failure. Two separate models are proposed. A numerical method for calculating crack-like zones up to macro fracture is proposed. The results of numerical fatigue experiments are presented. The operability of the single criterion model and calculation algorithm is shown on experimental results. The potential operability of the double criteria model was shown; the presence of two criteria that use different types of crack nucleation may result in cases when one of the criteria leads to crack growth while the other one does not and vice versa. Under a complex stress state in the proposed double criteria model the natural implementation of any of the considered crack development mechanisms is possible. Cracks of different types may be developing simultaneously in various parts of a specimen.

Keywords: Fatigue; Crack; Damage; Crack Development.

1. Introduction

In recent decades, entire classes of criteria have been constructed that relate the number of cycles before the initiation of fatigue damage (micro-cracks) with the amplitudes and maximum values in the cycle (or average) that characterize the uniform stress-strain state of the working part of the specimen in a fatigue test. A large number of stress-based criteria are based on a direct generalization of the S-N Wöhler-type curves described by Basquin-type relations in Basquin (1910), and based upon the results of fatigue tests. Reviews on this topic are given in Meggiolaro et al. (2007), Karolczuk et al. (2020) and Bourago et al. (2011).

* Corresponding author.
E-mail address: nikitin.alex@structuralintegrity.eu

10.1016/j.prostr.2020.11.027

In this paper we study the processes of fatigue damage zones development using the damage theory approach dating back to Kachanov (1958) and Rabotnov (1959). In the application to the cyclic loading and fatigue failure problems this approach was applied in Lemaitre and Chaboche (1994) and Marmi et al. (2009). Two models for the development of fatigue failure are proposed. First of them is based on the evolutionary equation for the damage function and utilizes the mechanism of normal crack micro-crack development. Second of them is associated with two different fatigue criteria. These criteria describe different crack development types. The model parameters are determined for various fatigue failure modes – low-cycle and high-cycle fatigue (LCF, HCF).

The following scheme of the amplitude fatigue curve is used. Up to value $N \sim 10^3$ the regime of repeated-static loading with amplitude slightly differing from the static tensile strength σ_B is realized. Further the fatigue curve (Wöhler curve) describes the modes of the LCF-HCF up to $N \sim 10^7$ with an asymptotic exit to the fatigue limit σ_u.

It should be noted that at present the idea of an explicit division of the classic Wöhler branch into two parts is in use – in fact, the LCF and the HCF. The boundary of transition region is determined not by the value of *N*, but by the value of the loading amplitude equal to the yield strength of the material σ_T, Shanyavskiy and Soldatenkov (2019), since this changes the physical mechanism of fatigue failure. The boundary of the repeated-static range $N \sim 10^3$ is rather arbitrary. However, in this paper we will keep the suggestion of the proposed model of damage development based on the scheme described above.

In order to match the first model with the well-known criteria for multiaxial fatigue failure, a stress-based criterion has been selected that describes the fatigue failure associated with the normal crack micro-cracks development. This is a modification of the Smith-Watson-Topper (SWT) criterion, Smith et al. (1970), described in Gates and Fatemi (2016), in which the amplitudes of maximum tensile stresses play a decisive role in the development of fatigue damage.

The second model is associated with the two well-known criteria for multiaxial fatigue failure. These criteria imply different micro-crack development types. The first one describes the fatigue failure associated with the tensile micro-cracks development; it is similar to the criterion from the first model. The second one describes the fatigue failure associated with the shear micro-cracks development. It is the stress-based Carpinteri–Spagnoli–Vantadori criterion, Carpinteri et al (2011). Under a complex stress state in the proposed complex model the natural implementation of any of the considered crack development mechanisms is possible. Cracks of different types may be developing simultaneously in various parts of a specimen.

For numerical simulation two simple specimens are used. Different loading regimes are applied to study the simultaneous action of the multiple criteria.

2. Kinetic equation for damage in LCH-HCF mode

Various criteria use different stress combinations to calculate an equivalent stress value. Some of them are based on normal stress components of a stress state while other are based on shear components. In this paper we are going to implement two criteria: one is based on a tensile micro-cracks which is the stress-based Smith–Watson–Topper, Gates and Fatemi (2016), the other one is based on a shear micro-cracks and implements the notion of a critical plane which is the stress-based Carpinteri–Spagnoli–Vantadori, Carpinteri et al. (2011).The considered models develop the damage model in case of cyclic loads, presented in Burago et al. (2019) for the description of damages during dynamic loading.

2.1. Generic equations

At first, let us introduce some variables that are used later.

We can write a generic fatigue fraction criterion corresponding to the left branch of the bimodal fatigue curve (Wöhler-type curve) in the following form:

$$\sigma_{eq} = \sigma_u + \sigma_L N^{-\beta} \tag{1}$$

From the condition of repeated-static fracture up to values of $N \sim 10^3$ by the method described in Bourago et al. (2011) it is possible to obtain the value $\sigma_L = 10^{3\beta}(\sigma_B - \sigma_u)$. In these formulas σ_B is the static tensile strength of the

material, σ_u is the classic fatigue limit of the material during a reverse cycle (asymmetry coefficient of the cycle R = -1), β is power index of fatigue curve.

From the fatigue fracture criterion we obtain the number of cycles before fracture at uniform stressed state:

$$N = 10^3 \left[(\sigma_B - \sigma_u) / (\sigma_{eq} - \sigma_u) \right]^{1/\beta} \tag{2}$$

In order to describe the process of fatigue damage development in the LCF-HCF mode, a damage function $0 \le \psi(N) \le 1$ is introduced, which describes the process of gradual cyclic material failure. When $\psi = 1$ a material particle is considered completely destroyed. Its Lame modules become equal to zero. The damage function ψ as a function on the number of loading cycles for the LCF-HCF mode is described by the kinetic equation:

$$\mathrm{d}\psi / \mathrm{d}N = B\psi^{\gamma} / (1 - \psi^{\alpha}) \tag{3}$$

where α and $0 < \gamma < 1$ are the model parameters that determine the rate of fatigue damage development. The choice of the denominator in this two-parameter equation, which sets the infinitely large growth rate of the zone of complete failure at $\psi \to 1$, is determined by the known experimental data on the kinetic growth curves of fatigue cracks, which have a vertical asymptote and reflects the fact of their explosive, uncontrolled growth at the last stage of macro fractures development.

An equation for damage of a similar type was previously considered in Marmi et al. (2009), its numerous parameters and coefficients were determined indirectly from the results of uniaxial fatigue tests. In our case, the coefficient B is determined by the procedure that is clearly associated with the selected criterion for multiaxial fatigue failure of one type or another. It has the following form.

The number of cycles to complete failure N at $\psi = 1$ is found from the equation for damage for a uniform stress state:

$$\begin{aligned} &\left[\psi^{1-\gamma} / (1-\gamma) - \psi^{(1+\alpha-\gamma)} / (1+\alpha-\gamma) \right]\Big|_0^1 = B\, N\Big|_0^N, \\ &N = \alpha / (1+\alpha-\gamma) / (1-\gamma) / B \end{aligned} \tag{4}$$

By calculating the value N from the fracture criterion (2) and from the solution of the equation for damage (4), we obtain the expression for the coefficient B :

$$B = 10^{-3} \left[(\sigma_{eq} - \sigma_u) / (\sigma_B - \sigma_u) \right]^{1/\beta} \alpha / (1+\alpha-\gamma) / (1-\gamma) \tag{5}$$

where the value σ_{eq} is determined by the selected mechanism of fatigue failure and the corresponding multiaxial criterion (1).

When $\sigma_{eq} \le \sigma_u$ fatigue failure does not occur, when $\sigma^{eq} \ge \sigma_B$ it occurs instantly.

2.2. Smith–Watson–Topper criterion

The criterion of multiaxial fatigue failure in the LCF-HCF mode with the development of normal-stress micro-cracks (stress-based SWT) corresponding to the left branch of the bimodal fatigue curve has the form:

$$\sqrt{\left\langle \sigma_{1_{\max}} \right\rangle \Delta\sigma_1 / 2} = \sigma_u + \sigma_L N^{-\beta} \tag{6}$$

where σ_1 is the largest principal stress, $\Delta\sigma_1$ is the spread of the largest principal stress per cycle, $\Delta\sigma_1/2$ is its amplitude. According to the chosen criterion only tensile stresses lead to failure, so it has the value $\langle\sigma_{1_{\max}}\rangle = \sigma_{1_{\max}} H(\sigma_{1_{\max}})$. Here $H(x)$ stands for the Heaviside step function.

Let us put down the following notation:

$$\sigma^n = \sqrt{\langle\sigma_{1_{\max}}\rangle \Delta\sigma_1 / 2} \tag{7}$$

Here the superscript *n* is not an exponent.

2.3. Carpinteri–Spagnoli–Vantadori criterion

The criterion of multiaxial fatigue failure in the LCF-HCF mode, including the concept of a critical plane (stress-based CSV), corresponding to the fatigue curve has the form:

$$\sqrt{(\langle\Delta\sigma_n\rangle/2)^2 + k_c^2(\Delta\tau_n/2)^2} = \sigma_u + \sigma_L N^{-\beta} \tag{8}$$

where $\Delta\tau_n/2$ is the amplitude of the tangential stress on the critical plane, where it reaches its maximum value, $\Delta\sigma_n/2$ is the amplitude of the normal (tensile) stress on the critical plane, $\langle\Delta\sigma_n\rangle = \Delta\sigma_n H(\sigma_{n_{\max}})$. Here, the shear fatigue limit τ_u for a pulsating cycle is additionally introduced at a cycle asymmetry coefficient of $R=-1$. In a simplified formulation, we can approximately accept $k_c \approx \sigma_u/\tau_u$ and $k_c \approx \sqrt{3}$. This criterion includes the mechanism of fatigue fracture with the formation of shear micro-cracks.

Let us put down the following notation:

$$\sigma^\tau = \sqrt{(\langle\Delta\sigma_n\rangle/2)^2 + 3(\Delta\tau_n/2)^2} \tag{9}$$

Here the superscript τ is not an exponent.

3. Algorithm for fatigue damage development calculation

The ANSYS software was used to calculate the loading cycle of a deformable specimen, supplemented by a code to calculate the damage equation and changes of elasticity modulus.

3.1. General approach to the damage function

To integrate the equation $d\psi/dN = B\psi^\gamma/(1-\psi^\alpha)$, the damage function ψ_k^t was sought at the nodes *k* of the computational grid for discrete time instants N^t. To calculate the damage equation, the value $\alpha = 1-\gamma$ was chosen by using an explicit expression for $\psi_k^{t+1}(\psi_k^t, \Delta N^t)$ that can be obtained by analytic integration:

$$\left[\psi^{1-\gamma}/(1-\gamma) - \psi^{2(1-\gamma)}/2/(1-\gamma)\right]\Big|_{\psi_k^t}^{\psi_k^{t+1}} = B_k N\Big|_{N^t}^{N^{t+1}} \tag{10}$$

With the denotations $(\psi_k^{t+1})^{1-\gamma} = x$, $q = 2(1-\gamma)B_k\Delta N^t + (\psi_k^t)^{1-\gamma} - 2(\psi_k^t)^{2(1-\gamma)}$ and $\Delta N^t = N^{t+1} - N^t$ the equation transforms to $x^2 - 2x + q = 0$ and its valid root $x = 1-\sqrt{1-q} < 1$. The damage parameter depends on the increment of the number of cycles ΔN^t as:

$$\psi_k^{t+1} = \left(1 - \sqrt{1 - \left[2(1-\gamma)B_k \Delta N^t + (\psi_k^t)^{1-\gamma} - 2(\psi_k^t)^{2(1-\gamma)}\right]}\right)^{1/(1-\gamma)} \tag{11}$$

Here increment value ΔN^t defined as follows. Based on the stress state data, the coefficient B_k is calculated for each node. After that, for each node, the following values are found

$$\Delta\tilde{N}_k^t = \left[\psi^{1-\gamma}/(1-\gamma) - \psi^{2(1-\gamma)}/2/(1-\gamma)\right]\Big|_{\psi_k^t}^{1} / B_k \tag{12}$$

that is corresponding to the number of cycles at which in the node k from its current level of damage and equivalent stress complete destruction will be achieved (damage is equal to 1). If the damage level in the considered node is less than the threshold ψ_0 (threshold $\psi_0 = 0.95$ is selected), then the value for this node $\Delta\tilde{N}_k^t$ is multiplied by a factor of 0.5. Otherwise, it is multiplied by a factor of 1. Thus, the step of incrementing the number of cycles for a given node is $\Delta N_k^t = 0.5(1 + H(\psi_k^t - 0.95))\Delta\tilde{N}_k^t$. Of all the ΔN_k^t values the smallest one is selected. The increment of the number of loading cycles for the calculation of the entire specimen is $\Delta N^t = \min_k \Delta N_k^t$. For each node, based on its current level of damage and equivalent stress, a new level of damage is estimated taking into account the calculated increment ΔN^t.

3.2. Material properties change

All elements are sorted out, for each of them the most damaged node is searched and according to its damage the mechanical properties of the element are adjusted:

$$\lambda(\psi_k^t) = \lambda_0(1 - \kappa\psi_k^t), \quad \mu(\psi_k^t) = \mu_0(1 - \kappa\psi_k^t) \tag{13}$$

Those elements that belong to nodes with damage $\psi = 1$ are removed from the calculation area and form a localized zone (crack-like) of completely destroyed material. The calculation ends when the boundaries of a completely damaged region exit to the specimen surface (macro destruction) or the evolution of this region stops.

3.3. Single criterion model

In the single criterion model we utilized Smith–Watson–Topper criterion. Our goal was to find the numerical coefficients of the criterion by matching the experimental and calculated fatigue curves for a specimen of certain geometry for a given loading amplitude and cycle asymmetry. Then using the obtained values, the experimental results on specimens of a different geometry and asymmetry coefficients were reproduced to find out the criterion operability.

3.4. Double criterion model

In the double criterion model we utilized both Smith–Watson–Topper and Carpinteri–Spagnoli–Vantadori criteria. The goal was to study the impact of different micro-crack development processes on the fatigue behavior of a specimen.

For it the following altering was made. At each node there are not one but two B values, namely B^n and B^τ. From (5) they have the forms:

$$\begin{aligned} B^n &= 10^{-3}\left[\left\langle \sigma^n - \sigma_u \right\rangle / (\sigma_B - \sigma_u)\right]^{1/\beta} \alpha / (1 + \alpha - \gamma) / (1 - \gamma), \\ B^\tau &= 10^{-3}\left[\left\langle \sigma^\tau - \sigma_u \right\rangle / (\sigma_B - \sigma_u)\right]^{1/\beta} \alpha / (1 + \alpha - \gamma) / (1 - \gamma) \end{aligned} \tag{14}$$

Consequently there are 2 values of damage parameter $\psi^n = f(B^n)$ and $\psi^\tau = f(B^\tau)$. At every step both ψ^n and ψ^τ are calculated for every node, then they are compared with each other at every node. When and where one of them becomes greater than 0 the other value is fixed to 0. It means that at every node the process that started first (via either SWT or SCV) prevails over the other one until the end of calculation process. Before the decisive moment both processes have equal rights to be the first one.

4. Calculation results

4.1. Single criterion model

To determine parameters of the proposed model and verify its performance, one of the fatigue in Marmi et al. (2009) has been performed numerically. From the condition of matching the experimental and calculated fatigue curves for a specimen of certain geometry for a given loading amplitude and cycle asymmetry the numerical coefficients were found. Using the obtained values, the experimental results on specimens of a different geometry and asymmetry coefficients were reproduced and calculation algorithm operability was confirmed.

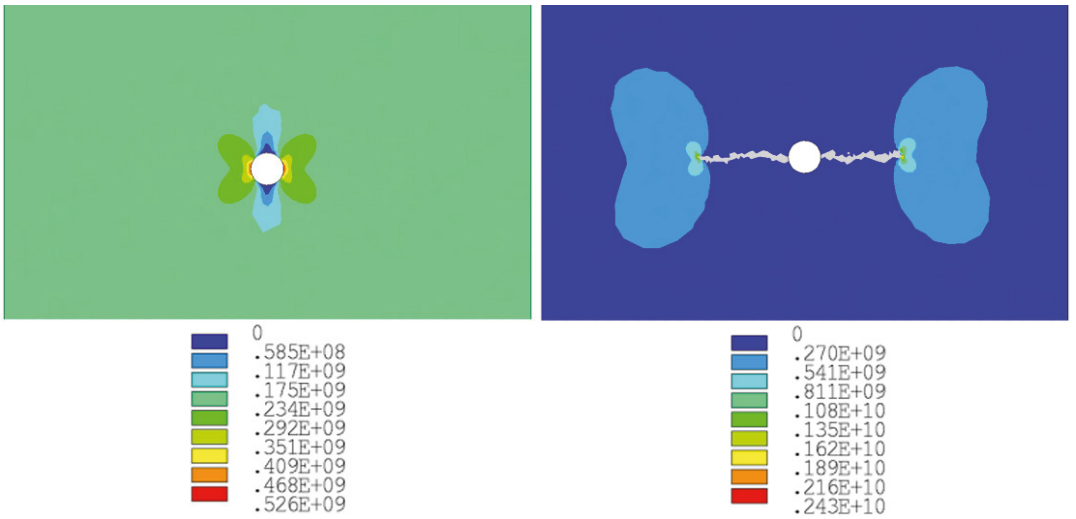

a) b)

Fig. 1. Specimen with a hole at R = -1:
a) emergence of a "quasi-crack", b) growth of a "quasi-crack".

Initial tests were conducted on a plate 100×25×1.57 mm in size with 1.56 mm diameter through hole in the ones center. Ratification tests were conducted on a V-notched specimen that has 15 mm width without a notch, thickness of 1.7 mm, the notch depth of 1.32 mm, the V-notch angle of 60 degrees and the notch radius of 0.675 mm. The cyclic loading of the upper and lower boundaries of the specimen with amplitude of 0.096 mm with the development of damage zones up to macroscopic destruction was simulated and matched with the results from Marmi et al. (2009). In the center of the plate there is a through hole with diameter of 1.56 mm.

Plate material – titanium alloy with strength and fatigue parameters σ_B = 1135 MPa, σ_u = 330 MPa, β = 0.31. Elasticity modulus of intact alloy are λ_0 = 77 GPa, μ_0 = 44 GPa. Fig. 1 and 3 show the lines of the effective stress level for the specimen with a hole (Fig. 1) and for the specimen with a notch (Fig. 3) in two states – before the fatigue quasi-crack initiation and at the moment when it has passed approximately halfway to macro-destruction.

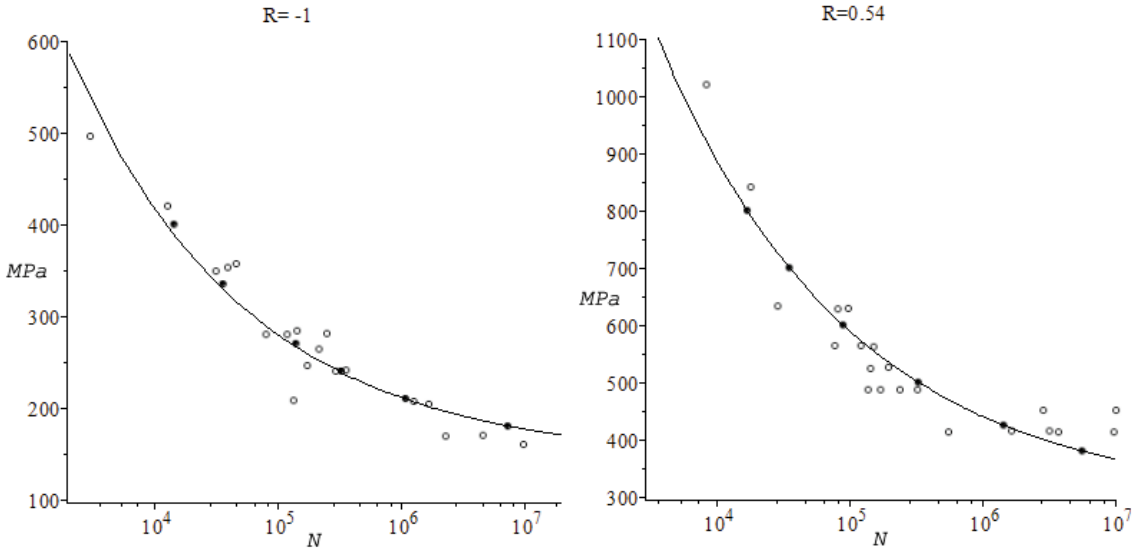

a) b)

Fig. 2. Fatigue curves $\sigma_{max}(N)$ for the specimen with a hole: ○ - real test points, ● - calculating points.

In Fig. 2 and 4 the results of real and computational experiments on constructing fatigue curves for specimens with a hole and a side notch are presented. Both real and calculated points represent the moment of a crack initiation. The curves in the figures approximate the experimental points. The calculations presented in Fig. 2-b almost exactly fit the approximation curve for the values of the model parameters. Utilizing these parameters, the fatigue curves presented in Fig. 2-a (specimen with a hole, R = 0.54) and in Fig. 3 (notched specimen, R = -0.5and 0.1). At Fig. 2-b, the calibration series, the relative error is 0. The average relative errors at Fig. 2-a, 3-a and 3-b are 1%, 7% and 6% respectively. The obtained satisfactory quality reproduction of real fatigue experiments indicates the efficiency and prospects of the model and calculation algorithm. The considered model represents the development of the damage model in case of cyclic loads, presented in Burago et al. (2019) for the description of damages during dynamic loading.

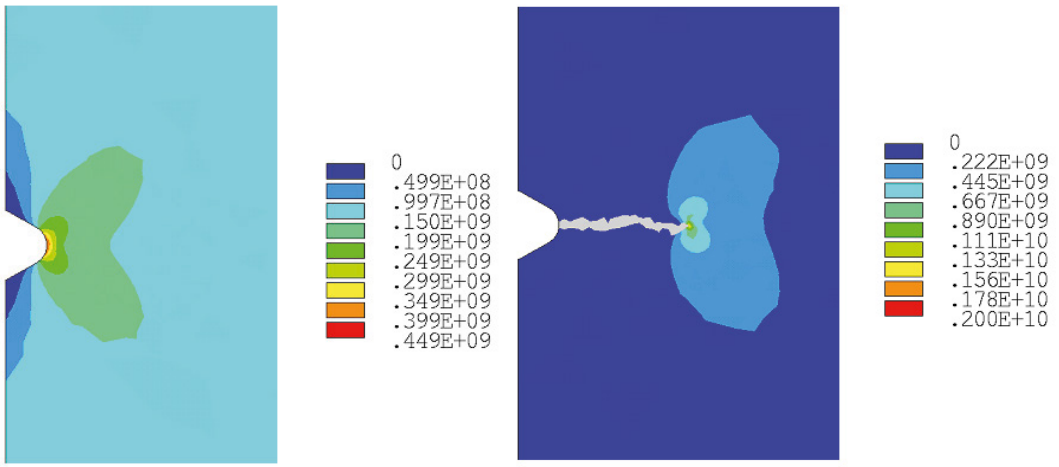

a) b)

Fig. 3. V-notched specimen at R = -0.5:
a) emergence of a "quasi-crack", b) growth of a "quasi-crack".

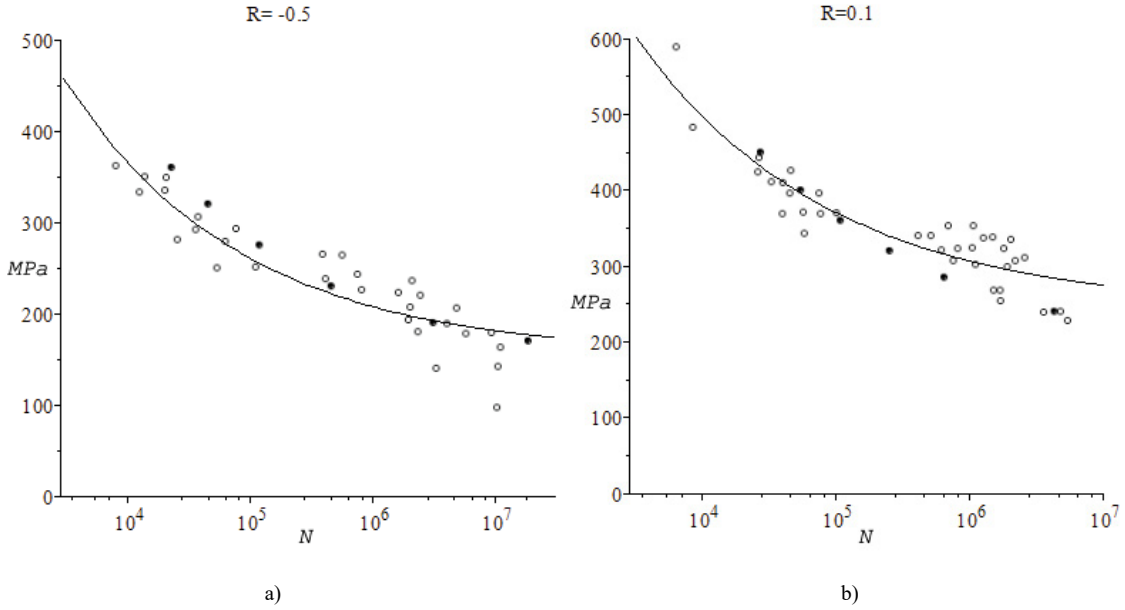

Fig. 4. Fatigue curves $\sigma_{max}(N)$ for V-notched specimen: ○ - real test points, ● - calculating points.

4.2. Double criterion model

A series of numerical experiments were conducted to determine the impact of the proposed double criterion scheme on fatigue behavior of a specimen. We studied a multi-axial case namely a torsion-compression stress-state.

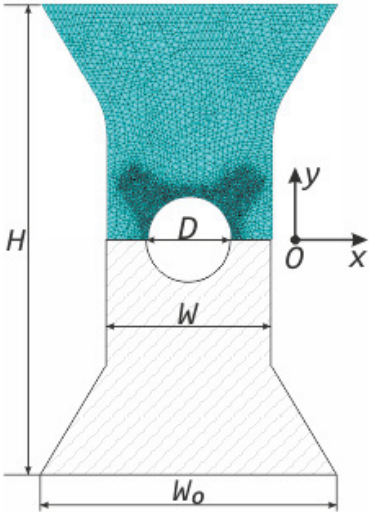

Fig. 5. Specimen geometry

All tests were conducted on a holed specimen, Fig. 5. Width at boundaries W_0 = 107 mm, main width W = 60 mm, height H = 170 mm, hole diameter D = 30 mm, thickness T = 1.75 mm. It should be noted that the numerical experiments were performed in three-dimensional space.

Due to symmetry of the specimen over Ox axis we decided to perform calculations only on the top half of the specimen. At that part the finite element grid is shown. We applied deformations at the top boundary of the specimen; due to its symmetry quasi-same deformations but in the opposite direction were applied at the bottom boundary, so at

the cross-section along Oxz there were no transverse (along Oy axis) deformations. In all numerical experiments all loads are in the same phase and their asymmetry ratios $R = 0.5$.

Plate material – titanium alloy with strength and fatigue parameters $\sigma_B = 1135$ MPa, $\sigma_u = 330$ MPa, $\beta = 0.31$. Elasticity modulus of intact alloy are $\lambda_0 = 77$ GPa, $\mu_0 = 44$ GPa.

Shear is applied along Ox axis which means that a positive shear deformation value corresponds to shift in the right-hand side direction. Tension and compression are applied along Oy axis. It means that a positive tension deformation corresponds to shift in the up direction and a positive compression deformation corresponds to shift in the down direction.

The first numerical experiment was on pure tension. The tension amplitude was 0.2 mm. The stress distribution before the crack initiation is presented at Fig. 6-a; the corresponding amount of cycles $N = 1.1 \cdot 10^5$. The stress distribution and the crack are presented at Fig. 6-b. The crack is marked with arrows, their direction show the type of the crack development process. Here the fracture process is provided by the development of normal-stress micro-cracks; the corresponding amount of cycles $N = 1.5 \cdot 10^5$.

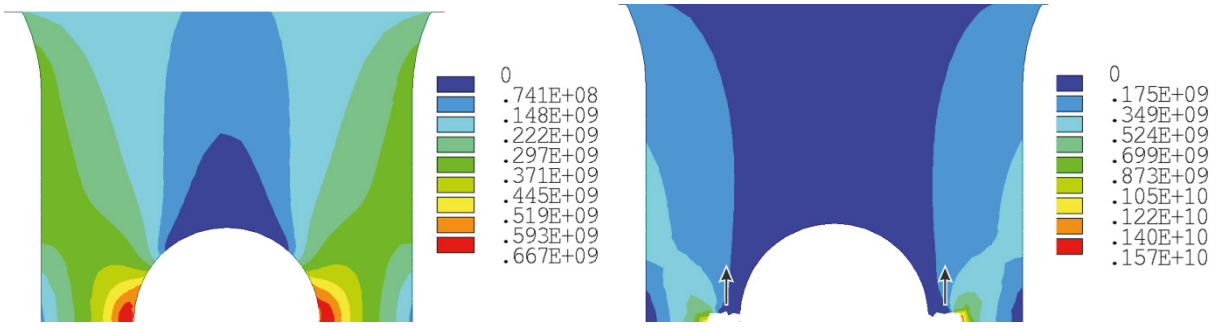

a) Before the crack initiation b) Crack growth process

Fig. 6. The numerical experiment on pure tension

The second numerical experiment was on pure shear. The shear amplitude was 0.5 mm. The stress distribution before the crack initiation is presented at Fig. 7-a; the corresponding amount of cycles $N = 6.2 \cdot 10^5$. The stress distribution and the crack are presented at Fig. 7-b. Again the crack was grown via the development of normal-stress micro-cracks; the corresponding amount of cycles $N = 7.2 \cdot 10^5$.

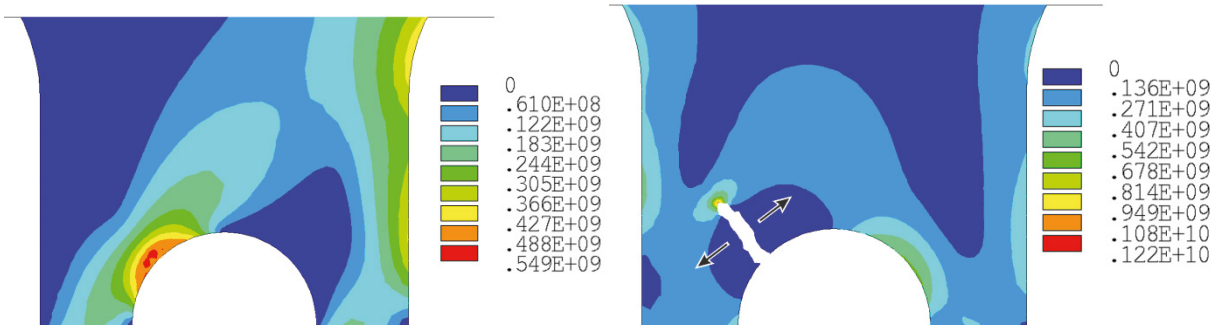

a) Before the crack initiation b) Crack growth process

Fig. 7. The numerical experiment on pure shear

The third numerical experiment comprises compression and shear. The compression amplitude was 0.06 mm and the shear amplitude was 0.5 mm. The stress distribution before the crack initiation is presented at Fig. 8-a; the corresponding amount of cycles $N = 9.0 \cdot 10^5$. The stress distribution and the crack are presented at Fig. 8-b. Here are

two crack, the left one was grown via the development of normal-stress micro-cracks while the right was grown via the shear-stress micro-cracks; the corresponding amount of cycles $N = 9.8 \cdot 10^5$.

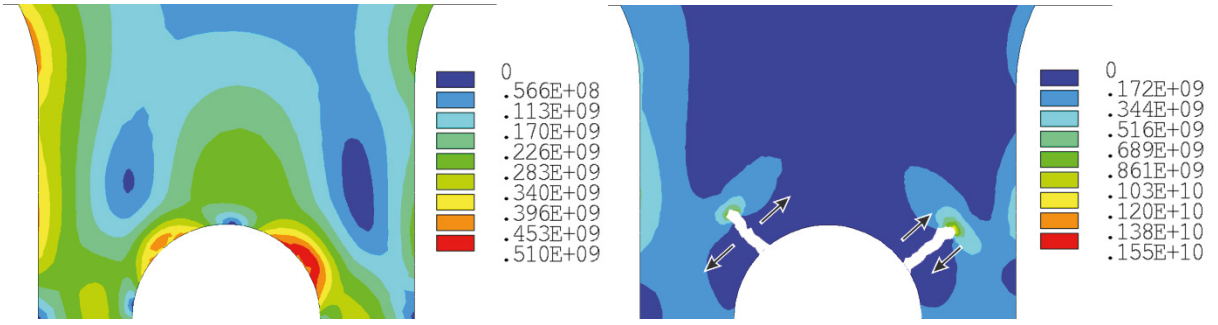

a) Before the crack initiation b) Crack growth process

Fig. 8. The numerical experiment on compression and shear

The fourth and the last numerical experiment again comprises compression and shear, but with different amplitudes. The compression amplitude was 0.1 mm and the shear amplitude was 0.5 mm. The stress distribution before the crack initiation is presented at Fig. 9-a; the corresponding amount of cycles $N = 3.2 \cdot 10^5$. The stress distribution and the crack are presented at Fig. 9-b. There is only one crack and it was grown via the shear-stress micro-cracks; the corresponding amount of cycles $N = 4.3 \cdot 10^5$.

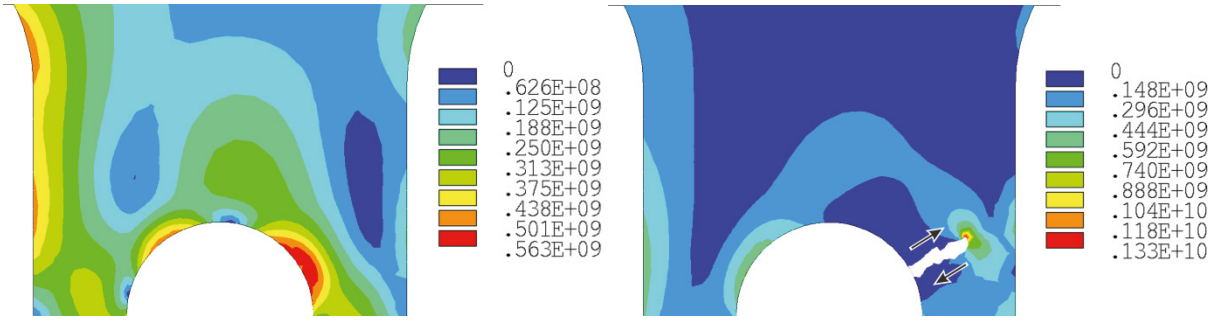

a) Before the crack initiation b) Crack growth process

Fig. 9. The numerical experiment on compression and shear

5. Conclusions

A kinetic model of cyclic loading damage development is proposed to describe the fatigue fracture process development. To determine the coefficients of the kinetic equation of damage, the known SWT criterion of multiaxial fatigue fracture was used. A numerical method for calculating crack-like zones up to macrofracture is proposed.

The single criterion model parameters are determined from the condition of matching the experimental and calculated fatigue curve for a specimen of a certain geometry at a given load amplitude and cycle asymmetry coefficient. Using the obtained values, the results of experiments on specimens of a different geometry and asymmetry coefficients were reproduced and the model and calculation algorithm performance was confirmed.

It was shown that the presence of two criteria that use different regimes of crack nucleation may result in cases when one of the criteria leads to crack growth while the other one does not and vice versa. Under a complex stress state in the proposed complex model the natural implementation of any of the considered crack development mechanisms is possible. Cracks of different types may develop simultaneously in various parts of a specimen.

Acknowledgments

The study was carried out with a grant from the Russian Science Foundation (project No. 19-19-00705).

References

Basquin, O. H., 1910. The exponential law of endurance tests. Proc. of the American society for testing and material 10, 625–30.

Meggiolaro, M. A., Miranda, A. C. and de Castro, J., 2007. Comparison among fatigue life prediction methods and stress-strain models under multiaxial loading. Proceedings of 19th Int. Congress of Mech. Eng.

Karolczuk, A., Papuga, J. and Palin-Luc, T., 2020. Progress in fatigue life calculation by implementing life-dependent material parameters in multiaxial fatigue criteria. Int. J. of fatigue 134, 1-13.

Bourago, N. G., Zhuravlev, A. B. and Nikitin I. S., 2011. Models of multiaxial fatigue fracture and service life estimation of structural elements. Mechanics of Solids 46, 828–38.

Kachanov, L. M., 1958. O vremeni razrushenija v usloviyah polzuchesty. Izv. AN SSSR OTN 8, 26–31.

Rabotnov, J. N., 1959. O mechanizme dlitel'nogo razrushenia. Voprosi prochnosti materialov i konstrukcij AN SSSR OTN, 5–7.

Lemaitre, J. and Chaboche, J. L., 1994. Mechanics of solid materials. Cambridge University Press, Cambridge, pp. 582.

Marmi, A. K., Habraken, A. M. and Duchene, L., 2009. Multiaxial fatigue damage modeling at macro scale of Ti6Al4V alloy. Int. J. of fatigue 31, 2031–40.

Shanyavskiy, A. A. and Soldatenkov, A. P., 2019. The fatigue limit of metals as a characteristic of the multimodal fatigue life distribution for structural materials. Procedia Structural Integrity 23, 63–8.

Smith, R. N., Watson, P. and Topper, T. H., 1970. A stress-strain parameter for the fatigue of metals. J. of Materials 5, 767–78.

Gates, N. and Fatemi, A., 2016. Multiaxial variable amplitude fatigue life analysis including notch effects. Int. J. of fatigue 91, 337–51.

Carpinteri, A., Spagnoli, A. and Vantadori, S., 2011. Multiaxial assessment using a simplified critical plane based criterion. Int. J. of Fatigue 33, 969–76.

Burago, N. G., Nikitin, I. S., Nikitin, A. D. and Stratula, B. A., 2019. Algorithms for calculation damage processes. Frattura ed Integrità Strutturale 49, 212–24.